




# The Interfacial Behavior Between Coke and Liquid Iron: A Comparative Study on the Influence of Coke Pore, Carbon Structure and Ash

MIN-MIN SUN,<sup>1</sup> JIAN-LIANG ZHANG,<sup>1,2</sup> KE-JIANG LI ,<sup>1,6</sup>  
HONG-TAO LI,<sup>1</sup> ZI-MING WANG,<sup>1</sup> CHUN-HE JIANG,<sup>1</sup>  
SHAN REN,<sup>3,7</sup> LI WANG,<sup>4</sup> and HANG ZHANG<sup>5</sup>

1.—School of Metallurgical and Ecological Engineering, University of Science and Technology Beijing, Beijing 100083, People's Republic of China. 2.—School of Chemical Engineering, The University of Queensland, St Lucia, QLD 4072, Australia. 3.—College of Material Science and Engineering, Chongqing University, Chongqing 400044, People's Republic of China. 4.—Beijing Jianlong Heavy Industry Group Co., Ltd, Beijing 100070, People's Republic of China. 5.—Modern Technology and Education Centre, North China University of Science and Technology, Tangshan 063009, People's Republic of China. 6.—e-mail: likejiang@ustb.edu.cn. 7.—e-mail: shan.ren@cqu.edu.cn

Identifying key factors governing the dissolution rate of metallurgical coke into liquid iron is important for sustainable developments of blast furnace iron-making. This study investigated the metallurgical coke dissolution into liquid iron by comparing the interfacial behavior between four carbonaceous materials and iron to clarify the influence of coke pore, carbon structure and ash. The wettability between coke and molten iron is reduced by the disorder of the carbon structure, and the presence of minerals can significantly reduce the rate of carburization with the dissolution breadth and depth of coke powder tablets reaching minimum values, 11 mm and 0.33 mm, respectively. The presence of pores significantly improves the dissolution rate, and the dissolution breadth and depth of coke slices increased to 16.5 mm and 0.97 mm, respectively. The main mechanism by which the pores accelerate the rate of metallurgical coke into the molten iron is to improve the contact area between the iron and the coke slices at high temperatures. The effect of the carbon structure and ash on the dissolution rate becomes weaker when there are pores in the coke.

## INTRODUCTION

An in-depth understanding of the dissolution behavior of carbonaceous materials into molten Fe-C alloys and the related reactions taking place across the carbon/melt interface are of great importance for various iron-making processes.<sup>1–3</sup> The blast furnace (BF) iron-making process still remains the primary iron production unit for the foreseeable future, even though intensive research has been undertaken in developing new iron-making technologies. The incremental improvement of BF efficiency and the resultant reduction of fuel consumption makes the BF iron-making process theoretically close to minimum energy consumption.<sup>4</sup> After a series of complicated reactions, the

coke remains in solid form throughout the lower zone of the BF, which guarantees the gas and liquid flow distribution. And it also provides the high temperature required for economic iron production, as well as the source of carbon in the liquid iron.<sup>5,6</sup> The effects of coke dissolution into liquid iron must be understood in order to predict how the BF will respond to the complex and changeable operating conditions, especially under the dual pressure of resource shortages and environmental pollution.<sup>7,8</sup>

Previous studies on coke dissolution mainly concentrated on the influence of the carbon structure, the coke mineral matter, and the properties of hot metal. The main conclusions are: (1) the carbon structure has little effect on the dissolution behavior of low-graphitizing carbon materials such as coal,

char and coke, etc., but the carburizing rate of graphite is obviously faster;<sup>9–11</sup> (2) coke mineral matter slows the carbon dissolution rate by forming mineral layers at the interface;<sup>12–15</sup> and (3) the presence of S and P in molten iron significantly reduces the dissolution rate of carbon.<sup>16–20</sup> Ohno et al. found that the effective area was decreased by the porosity of the coke, which has an obvious negative effect on the carburization reaction.<sup>21</sup> However, iron and carbon were solid phases at the beginning of the experiment, and the flow characteristics of molten iron at high temperature were not considered, as well as the developed open pores on the coke surface. Furthermore, there has been less research on the comparative influence of coke pores, carbon structure and ash. Coke is the only solid material remaining in the BF hearth. Porosity is an important feature of metallurgical coke, which is closely related to its physical and chemical properties.<sup>22,23</sup> In addition, the extracted tuyeres and hearth coke samples also show that a considerable part of slag/iron exists in the pores of the coke.<sup>24–26</sup> This indicates that liquid metal can enter into the interior of the coke through the connected pores formed after coke gasification, which accelerates the dissolution of carbon. The focus of this study is to clarify the different influences of coke pores, carbon structure and ash on carbon dissolution into liquid iron.

In this study, an ingenious experimental scheme was developed to study the influence of pore on coke dissolution, as well as the carbon structure and mineral matter. Through qualitative comparison and analysis between different influencing factors, the effects of coke pores, carbon structure and ash on the coke dissolution behavior were obtained. The experimental results show that, although poor wettability with liquid iron and high mineral matter content in coke slows down the dissolution of carbon, the increase of contact area caused by the presence of developed open pores weakens the effects of the first two.

## MATERIALS AND METHODS

### Experimental Sample

In order to compare the influence of coke pores, carbon structure and minerals on coke dissolution behavior, four samples ( $\phi 22 \text{ mm} \times 7 \text{ mm}$ ) were prepared (*C1*, *C2*, *C3*, *C4*), as shown in Fig. 1. Pure graphite powder (wt.% C > 99.99%) with particle sizes between 45  $\mu\text{m}$  and 74  $\mu\text{m}$  was pressed as *C1* (see Fig. 1a *C1*) as reported in previous work.<sup>27</sup> Coke powder with the same particle sizes before and after ash removal were pressed as *C2* and *C3* (see Fig. 1a *C2* and *C3*). A coke slice was prepared as *C4* (see Fig. 1a *C4*). The key differences between the four substrate materials are the crystallinity of carbon, the mineral content, and porosity characteristics inside the coke. The carbon structures of the samples were evaluated by X-ray diffraction,

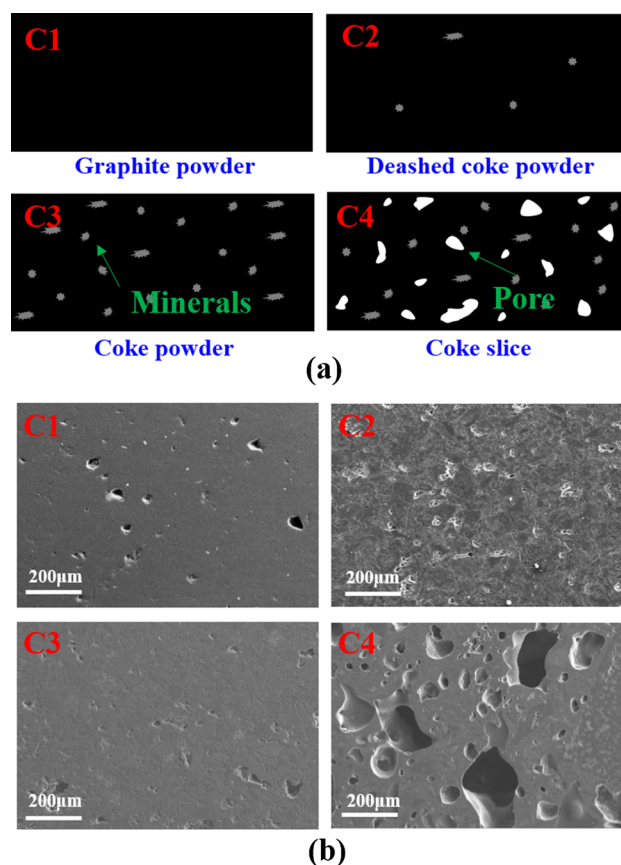


Fig. 1. Images of the four carbonaceous materials: (a) schematic diagrams show the main physical structures; (b) SEM images show the main surface morphologies.

and the  $L_c$  values were obtained with the Scherrer equation, which were 174.3  $\text{\AA}$  and 26.1  $\text{\AA}$  for graphite and coke, respectively. The differences of porosity were characterized by scanning electron microscopy (SEM) of the four different carbonaceous substrates, as shown in Fig. 1b. The de-ashed coke powder was prepared by dipping into a 6 vol.% HCl aqua solution and 40 wt.% HF aqua solution at 50°C with subsequent magnetic stirring for 2 h, then washing with distilled water and drying at 105°C.<sup>9</sup> After the pretreatment, the ash content decreased to less than 2 wt.%. The proximate analysis, ultimate analysis, and ash composition of the coke are shown in Table I.

### EXPERIMENTAL PROCEDURE

Pure iron (> 99.75%, 7 mm  $\times$  7 mm  $\times$  7 mm) was used for the carbon unsaturated iron samples, and *C1*–*C4* ( $\phi 22 \text{ mm} \times 7 \text{ mm}$ ) were used as substrates, in a 1700°C vacuum atmosphere box-type fiber heater furnace under 99.99% purity argon gas. Figure 2a shows a schematic diagram of the experimental device. In order to avoid the solid phase carburizing between the iron and carbon materials before melting, a corundum funnel was used as an

**Table I. The proximate analysis, ultimate analysis, and ash composition of coke****Proximate analysis of coke (mass%)**

Items	Moisture, ad	Ash, ad	Volatile, ad	Fixed Carbon, ad
Content	0.20	12.07	1.54	86.19

**Ultimate analysis of coke (mass%)**

Items	C	H	N	S	O
Content	84.58	0.78	1.12	0.64	0.63

**Composition of coke ash (mass%)**

Items	SiO <sub>2</sub>	Al <sub>2</sub> O <sub>3</sub>	Fe <sub>2</sub> O <sub>3</sub>	CaO	TiO <sub>2</sub>	MgO	K <sub>2</sub> O	SO <sub>3</sub>	P <sub>2</sub> O <sub>5</sub>
Before de-ashing	42.563	35.129	4.862	4.364	4.964	1.448	0.775	3.725	1.477
After de-ashing	41.480	33.963	4.838	3.251	9.355	0.837	0.668	3.203	1.356

ad air-dried basis.

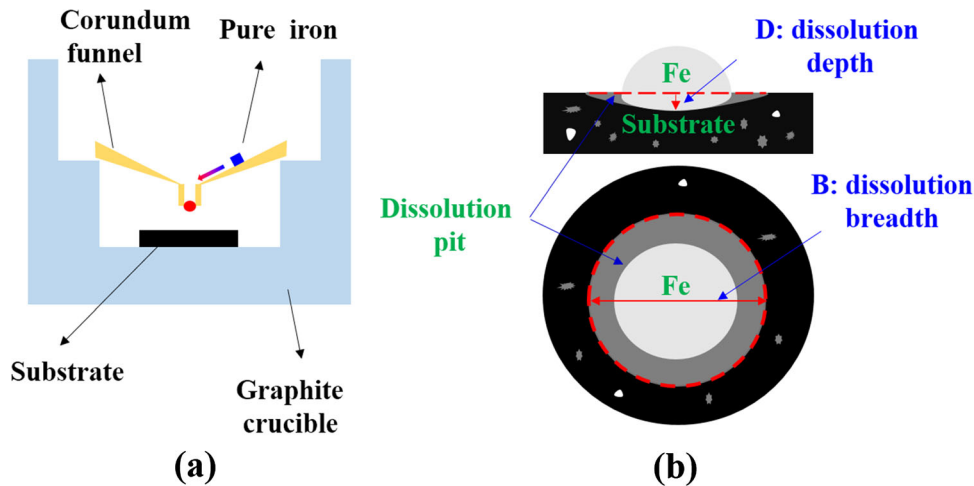


Fig. 2. Diagram of experimental apparatus: (a) schematic diagram of experiment device; (b) definition of dissolution depth  $D$  and dissolution breadth  $B$ .

iron droplet generating device. The heating rate were 25 K/min to 1173 K and 5 K/min to 1873 K. After holding for 90 min at 1873 K isothermally, the sample was rapidly cooled to room temperature with Ar. The interface between the iron droplets and the carbon substrate materials was observed to investigate the microstructural morphologies by SEM with an energy dispersive spectrometer (EDS). The experiments were repeated to observe the cross-sections of the solidified specimens after cutting and polishing. To characterize the differences in dissolution behavior of the four substrates more specifically, the definition of dissolution depth ( $D$ ) and dissolution breadth ( $B$ ) of the dissolution pits are shown in Fig. 2b.<sup>28</sup>

## RESULTS AND DISCUSSION

### Dissolution Behavior of Different Carbonaceous Substrates

Figure 3 shows images of the macroscopic and microscopic morphology after dissolution of the four carbonaceous substrates. It can be seen from Fig. 3a that the dissolution reaction occurred when liquid iron drops came into contact with the carbon substrates forming a circular pit. It was found that the surface of the Fe-C alloy carbonized by C1 and C2 formed some lamellar material, and they were well-developed graphite, as shown in Fig. 3bA. This may be a precipitation by the dissolved carbon in the liquid iron in the cooling process.<sup>29</sup> A part of

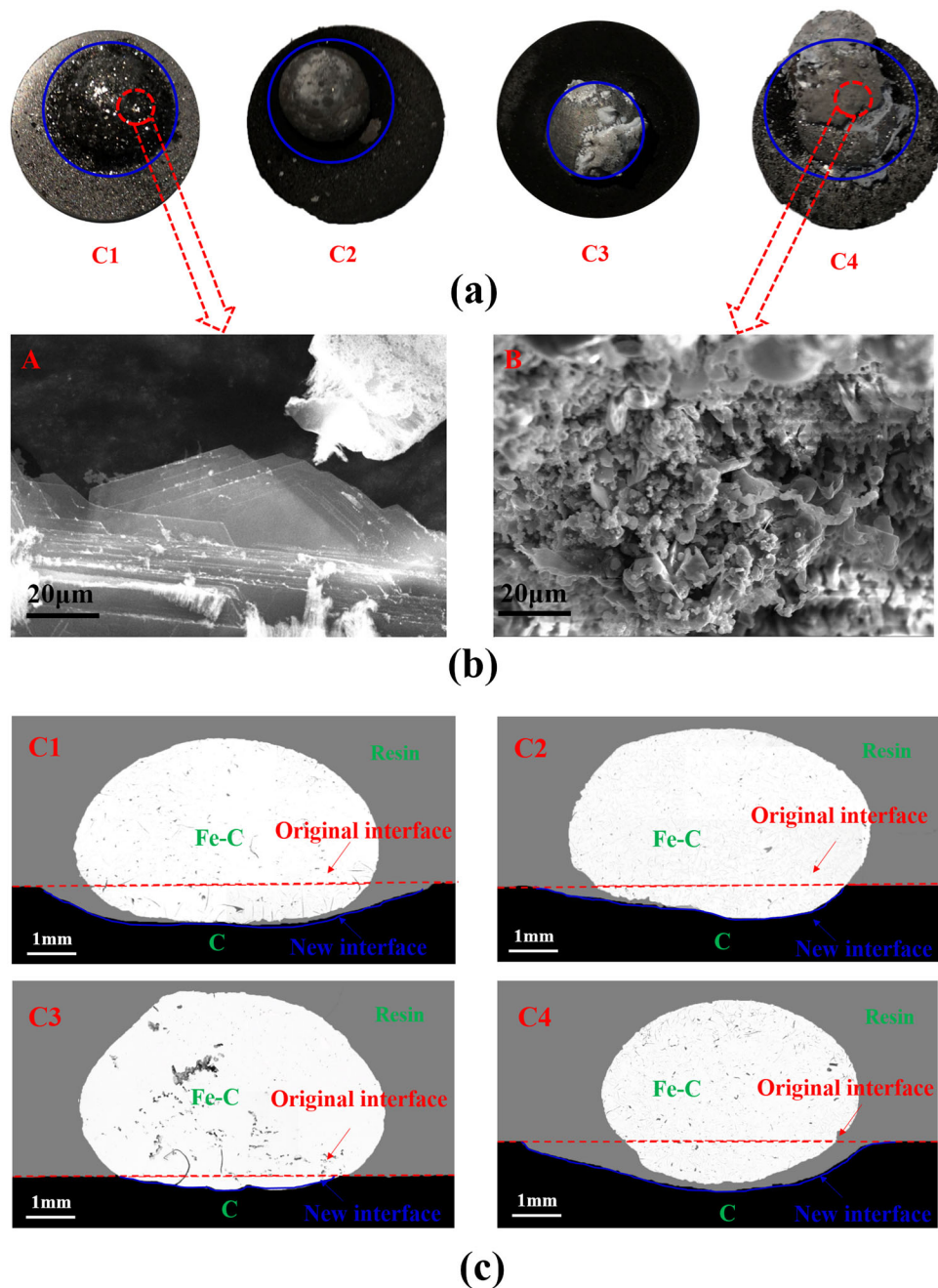


Fig. 3. Morphology of different carbonaceous substrates after dissolution: (a) macroscopic morphology images from top view; (b) microscopic observation of the surface phase of iron droplets; (c) backscatter SEM images for cross-sections of the solidified specimens.

agglomerates was observed on the surface of the Fe-C alloy carbonized by C3 and C4 (see Fig. 3bB). They were mainly minerals containing Ca and Al. The reason for the agglomerates is that the ash content in substrates C3 and C4 is 12.07 mass%, and the residual ash will agglomerate after the carbon is dissolved. Since the density of the mineral is less than iron, and the wettability between the mineral and molten iron is poor, they gradually migrate to the surface of the Fe-C alloy. Graphite crystals were also found when C4 was used. From the microscopic morphology of the interface after

dissolution, the dissolution pit of C1 is relatively uniform, and the dissolution of coke is not completely symmetrical due to the disorder of the carbon structure and the presence of pores, as shown in Fig. 3c. The dissolution pit of C3 is not obvious due to the mineral layer produced by ash accumulation. Although C4 has a low degree of minerals, its dissolution into liquid iron is close to that of C1 under the action of the pores.

Figure 4a shows the half-quantitative C content of Fe-C alloys carburized by different carbon

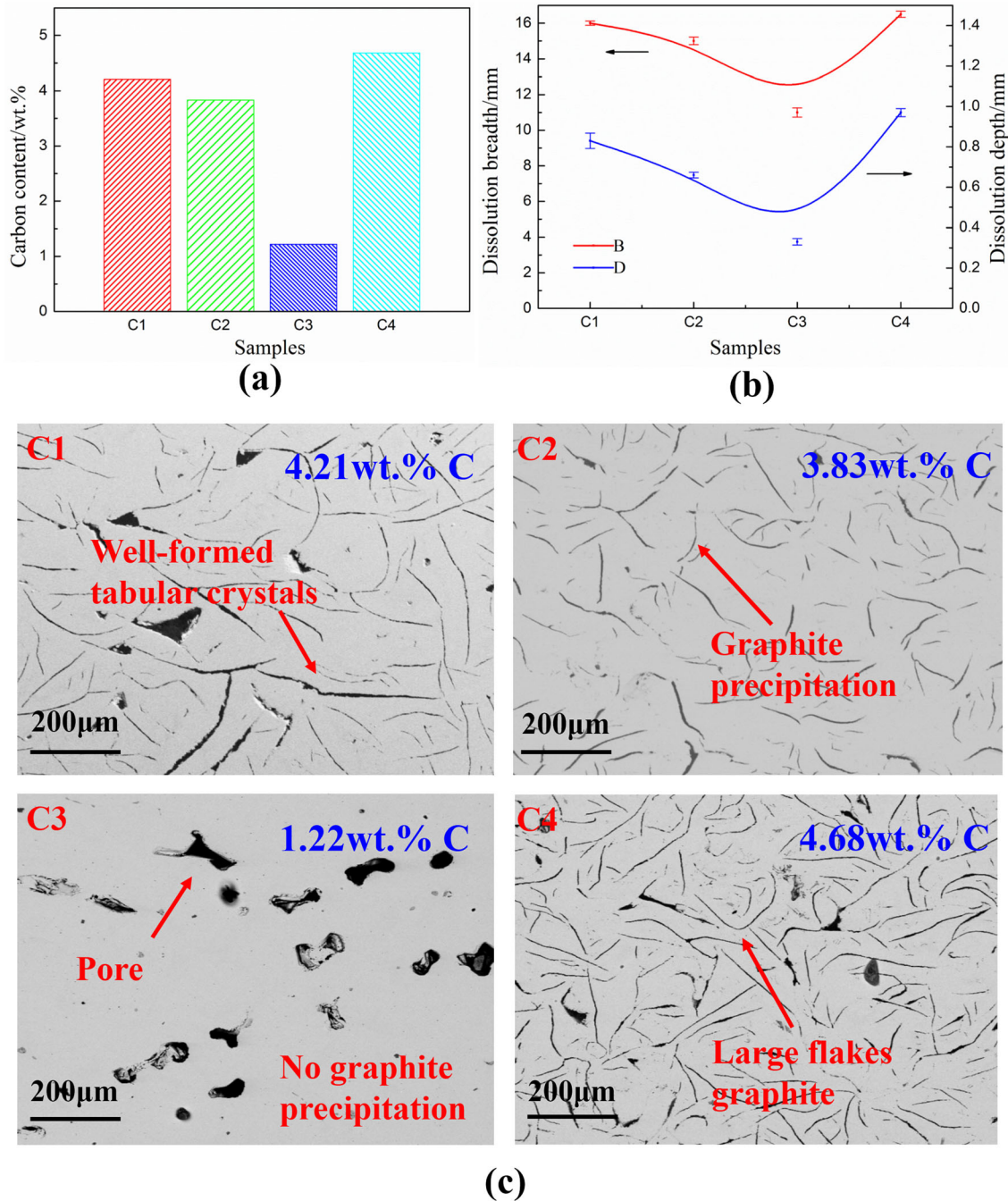


Fig. 4. Representation and comparison of dissolution behavior for different carbonaceous materials: (a) half quantitative C content of Fe-C alloys carburized by different carbon materials; (b) observed values of dissolution depth  $D$  and dissolution breadth  $B$ ; (c) backscattered electron imaging of Fe-C alloys carburized by different carbon materials.

materials with the aid of SEM-EDS surface scanning technology, which is closely related to the type of carbon material. The measured results of dissolution depth  $D$  and dissolution breadth  $B$  are shown in Fig. 4b. Similar to the results presented in Fig. 3, even though the lower ordered carbon structure has a negative effect on the carbon dissolution reaction,<sup>30</sup> poor wettability with liquid iron and the presence of sulfur has resulted in low levels of carbon dissolution for coke as compared to synthetic

graphite.<sup>9</sup> Due to the influence of the coke ash, both the dissolution breadth and depth of C3 reached minimum values, 11 mm and 0.33 mm, respectively. The dissolution behavior of C4 was better than that of C3, even being close to the result of graphite. The dissolution breadth of C4 is 16.5 mm (C1 is 16.0 mm), while the dissolution depth of C4 is 0.97 mm (C1 is 0.83 mm), which indicates that the pores of the coke have a great influence on its dissolution into liquid iron. In addition, the

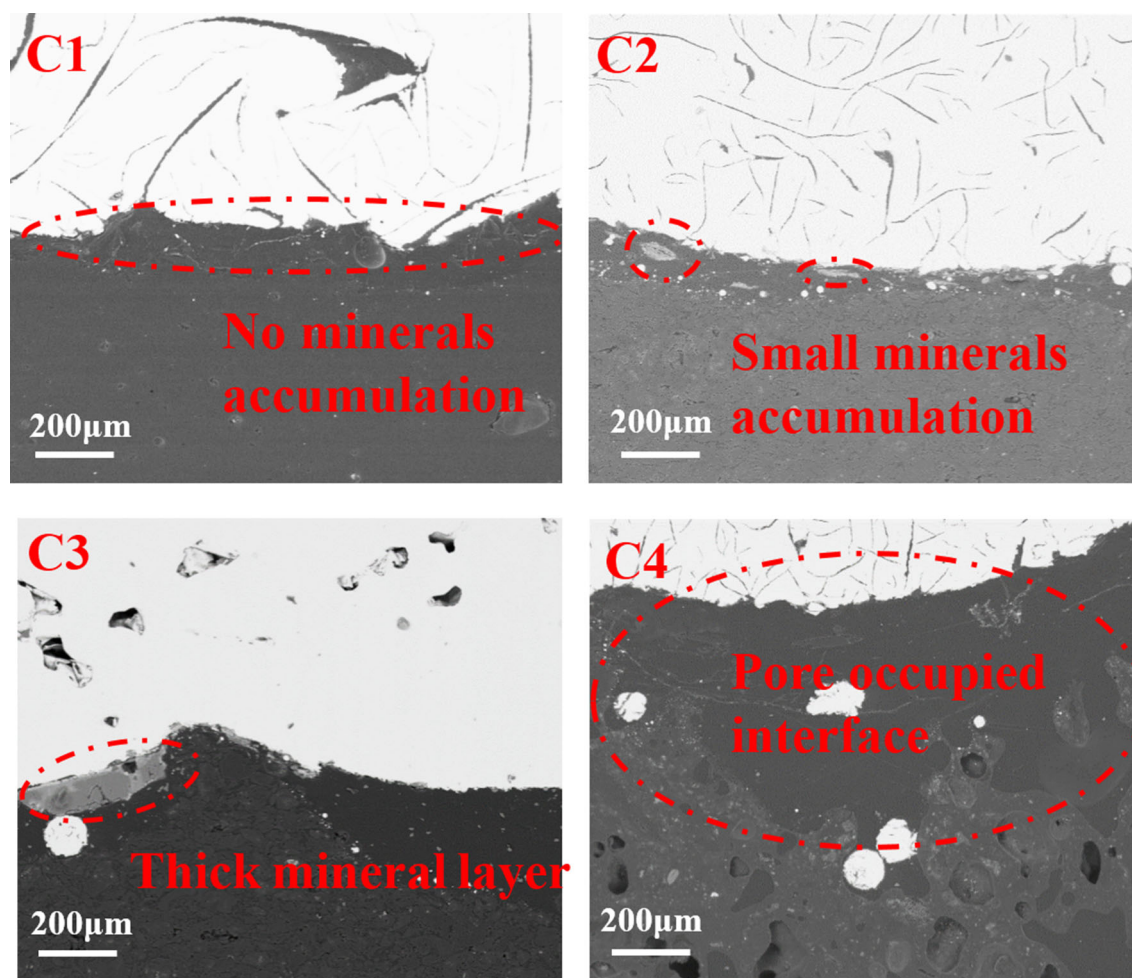


Fig. 5. Backscattered electron images of the carbon/iron interface after dissolution of different carbonaceous materials (C1, C2, C3, C4), mainly showing the distribution of minerals at the interface.

backscattered SEM images of Fe-C alloys carburized by different carbon materials are shown in Fig. 4c. Except for C3, well-formed flake graphite precipitated and was evenly distributed in the iron phase. No obvious graphite precipitation was observed in C3, but some bubbles were formed during recrystallization due to the dissolution of argon in the molten iron. The Ar solubility in the liquid iron at 1853 K was found to be  $1.095 \times 10^{-2}$  mL/100 g Fe. It reduces to  $5.45 \times 10^{-4}$  of Fe-0.5 mass% C alloy at 1803 K, while no Ar was detected in a similar experiment with an Fe-4.5 mass% C alloy at 1673 K.<sup>31</sup> The pores in the Fe-C alloy indicated the low amount of carbon dissolved in C3. The semi-quantitative detection revealed that C content (4.68 wt.%) in the Fe-C alloy carbonized by C4 was higher than that of the others. Through the above analysis, it can be seen that the coke dissolution rate has been reduced by the carbon crystalline and ash, while the pores in the coke significantly improved the dissolution rate. And the influence of carbon crystalline and minerals is no longer important compared to coke pore.

### Interfacial Products for Coke Dissolution into Liquid Iron

The interfacial layer formed due to the reaction between the carbonaceous materials and the liquid iron was characterized in detail to clarify the influence of mineral matter on the carburization rate. Backscattered electron images of the interfacial region are shown in Fig. 5. It can be seen that the accumulation of interface minerals has a strong relationship with the performance of the carbonaceous substrates. When pure graphite was used as the carburizing material, there was no mineral accumulation at the interface, while C2 had a small amount of mineral accumulation at the interface due to less mineral content after de-ashing. In C3, a large amount of mineral agglomeration occurred, and a thick mineral layer was formed at the carbon/iron interface. Different from C3, when the coke slice was used, the interface between the carbon and the metal was occupied by irregular connected pores, and no accumulation of minerals was found, which provides a better opportunity for iron/carbon contact.

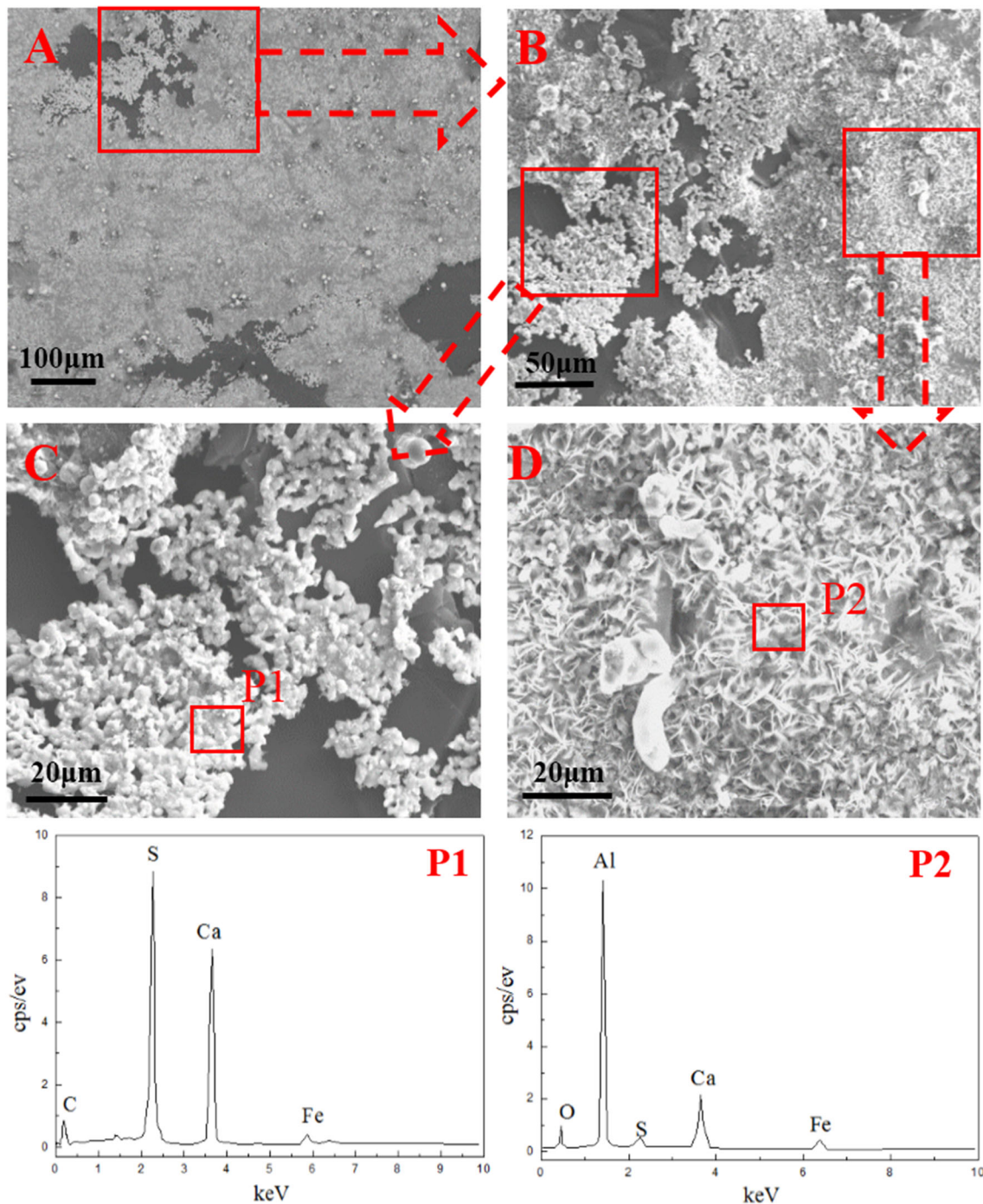
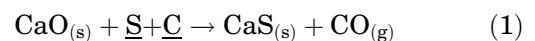


Fig. 6. SEM micrographs and EDS maps showing the interface between C3 and the metal: *A* and *B* are the interface morphologies at different magnifications; *C* and *D* are the morphologies of different minerals accumulated at the interface. EDS maps were taken from *P1* in *C* and *P2* in *D*.

Figure 6 shows the images of the interfacial region on the underside portion of the iron droplets carbonized by C3. As shown in Fig. 6a, the iron droplets are covered with a thick layer of minerals, and the interfacial products were different both in morphology and chemical composition (Fig. 6b). One of the interfacial products had a network or mesh-like structure (Fig. 6c), and EDS analysis showed that it was a kind of Ca/S complex, which

has an atomic ratio similar to calcium sulfide (CaS). From Table I, both the Ca element and the S element originated from coke inorganic mineral matter, and the formation of CaS can proceed via the following reaction:<sup>32</sup>



The dominant structure of other interfacial products is an open porous network of acicular particles

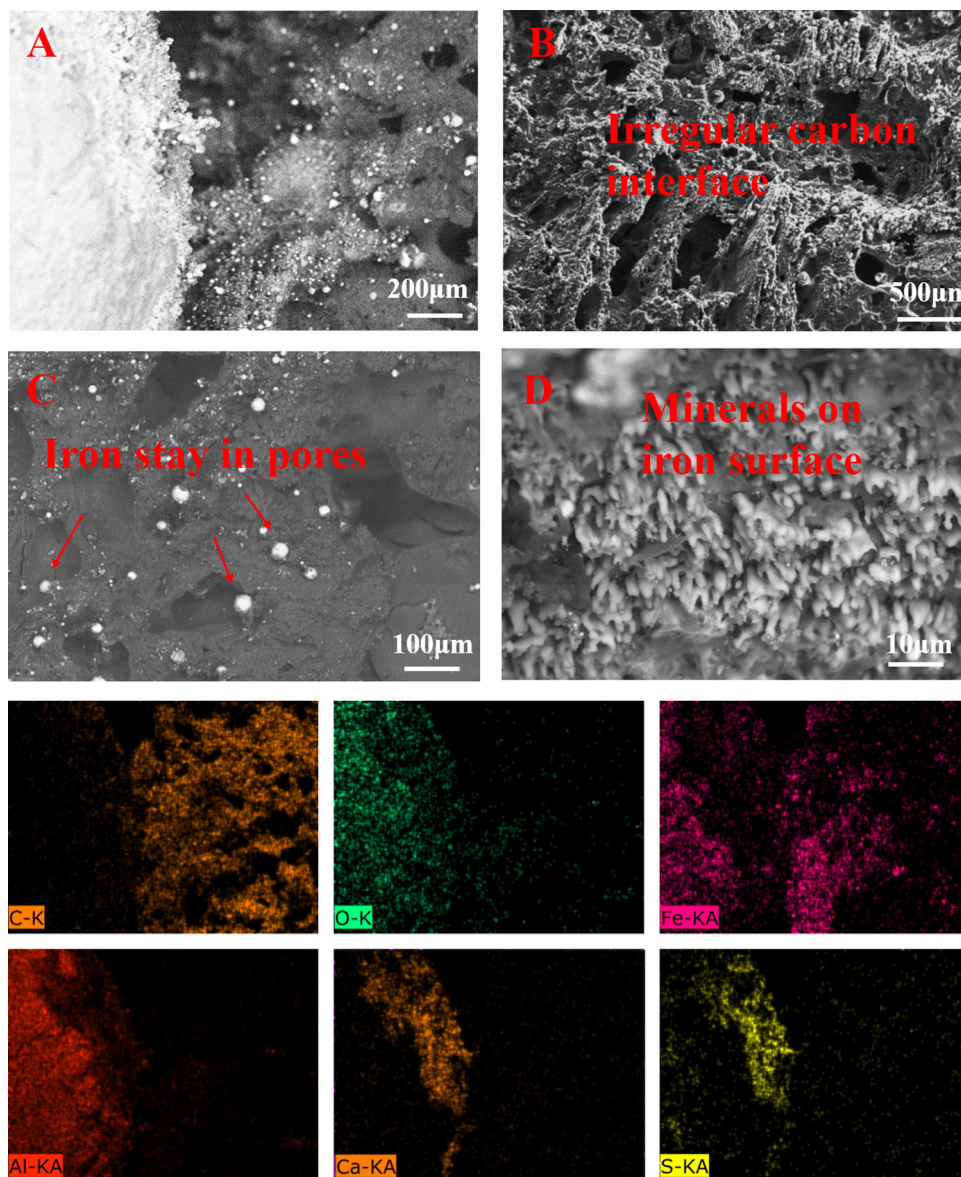


Fig. 7. SEM micrographs and EDS maps showing the interface between C4 and metal. *A* is the morphology of the iron/carbon junction after the reaction; *B* is the surface structure of the coke slice after the reaction; *C* is the morphology of iron droplets trapped in the pores of the coke; *D* is the topography of the minerals on the surface of the iron droplets. The EDS maps were taken from image *A*.

(needles) (Fig. 6d), the main elements of which are Ca, Al, and O. According to atomic ratio analysis, the acicular particles primarily consisted of alumina and calcium aluminates,  $\text{CaO}(\text{Al}_2\text{O}_3)_6$ .<sup>15</sup> There are also a few other calcium aluminates, CA2 and CA, because  $\text{Al}_2\text{O}_3$  is up to 35.129 mass%, while CaO is only 4.364 mass% in coke mineral matter. The formation of the mineral layer would block liquid iron from coming into contact with the carbon, which reduces the carbon dissolution into the liquid iron.

### Influence of Pores on Coke Dissolution into Liquid Iron

Figure 7 shows the SEM micrographs and EDS maps of the interface between C4 and the metal. It

can be seen from Fig. 7a that the pores in the coke after carburizing became excessively large and its connectivity was improved. Furthermore, the surface of the coke became extremely rough and irregular at higher magnifications, which provided a sufficient contact position for the reaction of the carbon and the molten iron at high temperatures. In addition, small Fe globules were observed in the surface and pores of the coke under backscattering SEM, which would allow liquid iron to freely come into contact with the carbon.<sup>12</sup> No obvious minerals were found on the surface of the coke. In contrast, a large amount of minerals was accumulated on the surface of the Fe-C alloy due to the smaller density of coke ash. The mapping analysis by EDS showed that the chemical composition of the mineral



products formed after carburizing with *C4* was the same as that with *C3*, which was mainly calcium sulfide (CaS), alumina (Al<sub>2</sub>O<sub>3</sub>) and calcium aluminates (CA6, CA2, CA).

The occurrence of dissolution reactions and the carburizing rate are mainly affected by the direct contact of liquid iron and carbon at high temperature. The main reason that the existence of pores can significantly accelerate the dissolution reaction of metallurgical coke can be summarized as:

1. The presence of pores causes the coke to dissolve unevenly, which provides a larger contact area for carburization.
2. Small Fe globules at the surface and connected pores of the coke allow liquid iron to freely come into contact with the carbon.
3. Minerals are more difficult to accumulate at the carbon/melt interface with the presence of pores, and the inhibition of coke dissolution by the interface mineral layer is weakened.

### Comparison Between the Influence of Coke Pores, Carbon Structure and Ash

The dissolution behavior of metallurgical coke is mainly affected by the physico-chemical properties of molten iron at high temperature and the structure and composition of the coke itself. Numerous studies have demonstrated that the existence of ash in carbonaceous materials does have a retarding effect on carbon dissolution. At the same time, the crystallite size, *L<sub>c</sub>*, would be a good additional criterion with which to assess carbon dissolution performance with comparable chemical compositions. However, little consideration has been given to the effect of pores in the coke structure, or to comparisons between the influence of coke pores, carbon structure and ash on dissolution rate.

Xu et al.<sup>33</sup> revealed that the carbon crystallite structure of the solid fuels used had a greater influence on dissolution behavior than their ash properties. However, the effect of pores was not taken into account in the selection of lumpy fuel samples (30 mm × 30 mm × 60 mm), and the effects of carbon structure and ash content could not be considered separately. Ko-ichiro et al.<sup>9</sup> proved that ash in charcoal (under 200 μm) has a stronger effect on carburization behavior than carbon crystallinity with the help of heat-treated charcoal samples which were additionally treated with acid solutions. Tsuey et al.<sup>34</sup> added carbonaceous material of 1.18–2.36 mm size fraction to the iron bath and found that there is no obvious effect of crystallite size and anisotropic carbon content on the rate of carbon dissolution. Ash composition is a dominant factor that influences the rate of carbon dissolution. Neither Ko-ichiro and S.Tsuey fully considered the physical and chemical properties of coke influencing carbon dissolution into liquid iron. The research in this paper comprehensively

considers the influence of coke pores, carbon structure, and ash on its dissolution behavior in molten iron. In comparison with graphite, the slowing effect of the disordered carbon structure on carburization was demonstrated. The dissolution behavior of the coke powder with and without de-ashing treatment indicated that the production of a mineral layer at the interface reduced the contact of the carbon material with liquid iron at high temperature, thereby inhibiting the continuation of carburization reaction. Finally, using coke slices, it was found that the carburizing rate of coke is close to that of graphite, even under the simultaneous reducing effect of a disordered carbon structure and the ash. This indicated that the influence of coke pores on the dissolution is very obvious, far exceeding that of the carbon structure and ash. The microstructure of coke needs to be considered in any proposed explanation for the variation in carburization rates.

### CONCLUSION

The dissolution behavior of four carbonaceous materials were studied to compare the influence of pores, the carbon structure, and ash on metallurgical coke dissolution into liquid iron. The disorder of the carbon structure and the presence of minerals can significantly reduce the rate of carbon dissolution, and both the dissolution breadth and depth of *C3* reached minimum values, 11 mm and 0.33 mm, respectively. In industrial coke, the presence of developed pores significantly improves the dissolution behavior, with the dissolution breadth and depth of *C4* increasing to 16.5 mm and 0.97 mm, respectively.

The main mechanism by which the pores accelerate the dissolution rate of metallurgical coke into the molten iron is to improve the contact area between the molten iron and the coke slice at high temperatures. On the one hand, the presence of pores causes uneven dissolution of coke, while the pores also provide sufficient space for the flow of molten iron, which increases the contact between the iron and the coke. On the other hand, minerals cannot accumulate at the iron/carbon interface, and the inhibition of coke dissolution by the interface mineral layer is weakened by the presence of pores. The dissolution rate of coke is close to that of graphite even with the disordered carbon structure and mineral matter. The influence of coke pores on dissolution is very obvious, far exceeding that of the carbon structure and ash. The microstructure of coke needs to be considered in any proposed explanation for the variation in carburization rates.

### ACKNOWLEDGEMENTS

This work was part of a research project named "The dissolution behavior and carburizing ability of coke dissolution in hot metal" supported by the National Science Foundation of China [51774032], the National Key Research and Development

Program of China [2017YFB0304300 & 2017YFB0304303], the National Science Foundation for Young Scientists of China (51804025), the Chinese Fundamental Research Funds for the Central Universities [FRF-TP-17-086A1].

## REFERENCES

1. H.W. Gudenau, J.P. Mulanza, and D.G.R. Sharma, *Steel Res.* 61, 97 (1990).
2. B. Cusack, G. Hardie, and P. Burke, European Ironmaking Cong. Glasgow, 1991.
3. J. Keogh, G. Hardie, D. Philip, and P. Burke, *AIME 50th Ironmaking Conference Proceedings*, Washington, 1991.
4. M. Hallin, *Ishii Symposium on Sustainable Ironmaking*, CCSD, Sydney, Australia. 2006.
5. Y. Omori, Blast furnace phenomena and modelling. (Committee on reaction within blast furnace, 1987), pp. 98-124.
6. X. Wang, *Metallurgy of Iron and Steel, Part I: Ironmaking*, 2nd ed. (Beijing: Metallurgical Industry Press, 2013), pp. 36-42.
7. T. Murakami, M. Ohno, K. Suzuki, K. Owaki, and E. Kasai, *ISIJ Int.* 57, 1928 (2017).
8. C.S. Nguyen, K. Ohno, T. Maeda, and K. Kunitomo, *ISIJ Int.* 57, 1491 (2017).
9. K. Ohno, A. Babich, J. Mitsue, T. Maeda, D. Senk, and H.W. Gudenau, *ISIJ Int.* 52, 1482 (2012).
10. C. Wu, R. Wiblen, and V. Sahajwalla, *Metall. Mater. Trans. B* 31, 1099 (2000).
11. M. Chapman, *Insoluble oxide product formation and its effect on coke dissolution in liquid iron*, University of Wollongong, Doctoral Dissertation, 64 (2009).
12. S.T. Cham, R. Khanna, V. Sahajwalla, R. Sakurovs, and D. French, *ISIJ Int.* 49, 1860 (2009).
13. B.J. Monaghan, M.W. Chapman, and S.A. Nightingale, *Steel Res. Int.* 81, 829 (2010).
14. R. Khanna, V. Sahajwalla, B. Rodgers, and F. McCarthy, *Metall. Mater. Trans. B* 37, 623 (2006).
15. M.W. Chapman, B.J. Monaghan, S.A. Nightingale, J.G. Mathieson, and R.J. Nightingale, *Metall. Mater. Trans. B* 39, 418 (2008).
16. V. Sahajwalla and R. Khanna, *Metall. Mater. Trans. B* 31, 1517 (2000).
17. V. Sahajwalla and R. Khanna, *Acta Mater.* 50, 663 (2002).
18. F. McCarthy, R. Khanna, V. Sahajwalla, and N. Simento, *ISIJ Int.* 45, 1261 (2005).
19. F. McCarthy, V. Sahajwalla, J. Hart, and N. Saha-Chaudhury, *Metall. Mater. Trans. B* 34, 573 (2003).
20. Y. Deng, J. Zhang, and K. Jiao, *ISIJ Int.* 24, 659 (2018).
21. K. Ohno, S. Miura, T. Maeda, and K. Kunitomo, *ISIJ Int.* 59, 655 (2019).
22. K. Li, R. Khanna, J. Zhang, Z. Liu, V. Sahajwalla, and T. Yang, *Fuel* 133, 194 (2014).
23. S. Gupta, D. French, R. Sakurovs, M. Grigore, H. Sun, and T. Cham, *Prog. Energy Combust. Sci.* 34, 155 (2008).
24. K. Li, J. Zhang, Z. Liu, M. Barati, J. Zhong, and M. Wei, *Metall. Mater. Trans. B* 46, 1104 (2015).
25. K. Li, J. Zhang, M. Sun, C. Jiang, Z. Wang, and J. Zhong, *Fuel* 225, 299 (2018).
26. M. Sun, J. Zhang, K. Li, K. Guo, H. Wang, and Z. Wang, *Metall. Mater. Trans. B* 49, 2611 (2018).
27. M. Sun, J. Zhang, K. Li, S. Ren, Z. Wang, and C. Jiang, *JOM* 71, 4305 (2019).
28. C.S. Nguyen, K. Ohno, T. Maeda, and K. Kunitomo, *ISIJ Int.* 56, 1325 (2016).
29. S.S. Gornostayev, T.M. Fabritius, O. Kerkkonen, and J.J. Härkki, *Int. J. Miner. Metall. Mater.* 19, 478 (2012).
30. K. Ohno, T. Maeda, K. Nishioka, and M. Shimizu, *ISIJ Int.* 50, 53 (2010).
31. Y. Sasaki, Y. Kashiwaya, and K. Tokuchi, *Metall. Mater. Trans. B* 31, 216 (2000).
32. M.W. Chapman, B.J. Monaghan, S.A. Nightingale, J.G. Mathieson, and R.J. Nightingale, *Metall. Mater. Trans. B* 42, 642 (2011).
33. R. Xu, J. Zhang, W. Wang, H. Zuo, Z. Xue, and M. Song, *J. Iron. Steel Res. Int.* 25, 298 (2018).
34. S.T. Cham, V. Sahajwalla, R. Sakurovs, H. Sun, and M. Dubikova, *ISIJ Int.* 44, 1835 (2004).

**Publisher's Note** Springer Nature remains neutral with regard to jurisdictional claims in published maps and institutional affiliations.